Cancer Biol Med 2025. doi: 10.20892/j.issn.2095-3941.2024.0434

ORIGINAL ARTICLE

Neoepitope BTLA^{P267L}-specific TCR-T cell immunotherapy unlocks precision treatment for hepatocellular carcinoma

Fang Liu[1,2,3], Hua Chen[4], Suxin Wu[1,2,3], Chenlu Zhu[1,2,3], Mingji Zhang[3,5], Wei Rui[4], Dong Zhou[3,5], Yang Wang[2,3], Xin Lin[4], Xueqiang Zhao[4], Yunbin Ye[2,3]

[1]School of Basic Medical Sciences, Fujian Medical University, Fuzhou 350122, China; [2]Laboratory of Immuno-Oncology, Clinical Oncology School of Fujian Medical University, Fujian Cancer Hospital, Fuzhou 350014, China; [3]Fujian Key Laboratory of Translational Cancer Medicine, Fuzhou 350014, China; [4]School of Basic Medical Sciences, Tsinghua University, Beijing 100084, China; [5]The Department of Hepatopancreatobiliary Surgery, Clinical Oncology School of Fujian Medical University, Fujian Cancer Hospital, Fuzhou 350014, China

ABSTRACT

Objective: The high heterogeneity of hepatocellular carcinoma (HCC) renders traditional therapies unable to effectively activate the patient's immune system to combat tumors. Patients with advanced HCC and T cell functional deficiencies may benefit more from cellular immunotherapy, especially tumor neoepitope-targeted T cell receptor (TCR)-T cells. Neoepitopes with strong immunogenicity provide precise targets for HCC, further enhancing the efficacy of cellular immunotherapy.

Methods: A scalable workflow for identifying neoepitopes from 7 HLA-A*02:01-restricted patients with HCC was established based on whole exome sequencing and bioinformatics analyses, followed by identification of neoepitope-specific TCRs through tetramer-based screening and single-cell TCR cloning technology, which were further validated in the JC4 cell model. The cytotoxicity of CD8$^+$ TCR-T cells was evaluated in neoepitope-positive tumor cell lines or NCG mice.

Results: Ten specific neoepitopes were identified, among which neoepitope B and T lymphocyte attenuator^{P267L} [BTLA^{P267L} (SLNHSVIGL)] exhibited advantageous properties as a potential tumor target. Three TCRs (85-3, 126-5, and 52-3) were confirmed to specifically recognize the neoepitope BTLA^{P267L}, while no cross-recognition of irrelevant or wild-type epitopes was observed. Activated BTLA^{P267L}-specific CD8$^+$ TCR-T cells released extensive perforin, granzyme B, IFN-γ, and TNF-α *in vitro*, thereby inducing strong cytotoxic effects against BTLA^{P267L}-positive T2 or HCC cell lines. BTLA^{P267L}-specific CD8$^+$ TCR-T cells mediated robust tumor regression due to long-lasting survival and released perforin without causing significant cytotoxic effects on normal organs in murine experiments.

Conclusions: This preclinical study demonstrated the beneficial effects of neoepitope BTLA^{P267L}-specific TCR-T cell immunotherapy, unlocking a novel strategy for personalized precision therapy in HCC.

KEYWORDS Neoepitope; T cell receptor-T cell; immunotherapy; hepatocellular carcinoma

Introduction

According to a report from the National Cancer Center (NCC) of China in 2024, the outlook for hepatocellular carcinoma (HCC) is not optimistic. The incidence of HCC ranks fourth, while the mortality rate ranks second[1]. Because of the complicated pathogenesis, dormant early symptoms, and rapidly developing processes, most patients with HCC are diagnosed in an advanced stage, resulting in a 5-year survival rate of < 5%. These facts highlight the limitations of traditional treatment and underscore the urgent need for developing new treatment strategies. Cellular immunotherapy has ushered in a new era in cancer treatment with chimeric antigen receptor (CAR)- and T cell receptor (TCR)-T cells as representatives[2]. The role of CAR-T cells in hematologic tumors is apparent. However, the effectiveness of CAR-T cells in treating solid tumors is unsatisfactory. Several clinical trials have shown that the efficacy of CAR-T cells has improved with the continuous advances in biotechnology and the side effects of CAR-T cell therapy are also manageable. Notably,

Correspondence to: Yunbin Ye and Xueqiang Zhao
E-mail: zjyunbin@fjmu.edu.cn and zhaoxueqiang@tsinghua.edu.cn
ORCID ID: https://orcid.org/0000-0002-0256-987X and https://orcid.org/0009-0003-3602-117X
Received October 4, 2024; accepted January 23, 2025; published online April 9, 2025.
Available at www.cancerbiomed.org
©2025 The Authors. Creative Commons Attribution-NonCommercial 4.0 International License

Glypican-3 (GPC3)-targeted CAR-T cells (C-CAR031), which were developed by AbelZeta (Rockville, MD, USA) and AstraZeneca (Cambridge, Eng., UK), have made significant breakthroughs in the treatment of HCC. However, the limited antigen recognition and the poor infiltration of CAR-T cells into the tumor microenvironment continue to limit application in solid tumors[3-5]. In contrast, TCR-T cells recognize cell surface and intracellular antigens (90%) presented by human leukocyte antigen (HLA), facilitating infiltration of TCR-T cells into solid tumors. Moreover, the epitope density required to activate TCR-T cells (1–50 epitopes per cell) is much lower than the epitope density required for CAR-T cells (10^3 epitopes per cell), suggesting that TCR-T cells are better at killing tumor cells with low-abundance antigens[6]. Therefore, we believe that TCR-T cell therapy warrants further investigation in the treatment of solid tumors.

TCR diversity serves as a pivotal anti-tumor mechanism for T cells, which typically exhibits a normal distribution among healthy individuals and enables T cells to swiftly respond upon encountering antigens, thereby preventing "tumor escape". However, with aging or the occurrence of tumors, TCR diversity decreases and the proportion of clonal distribution increases. A reduction in TCR diversity causes insufficient generation or impaired function of tumor antigen-specific T cells. To alleviate the concerns, engineered TCR-T cell immunotherapy has been developed and tumor antigen-specific TCR-T cells are transfused back into patients with cancer to ameliorate the TCR deficiency. Several clinical trials on TCR-T cell immunotherapies for treating HCC are ongoing or completed, including NCT04745403, NCT05339321, NCT03899415[7,8], NCT03634683[9], NCT04677088, NCT02686372, NCT02719782[10], NCT04368182, NCT03971747[11], NCT03132792[12], NCT03159585, NCT02869217, and NCT01967823. Most of these clinical trials have focused on viral antigens [e.g., hepatitis B virus (HBV)] or tumor-associated antigens [e.g., alpha-fetoprotein (AFP) and New York esophageal squamous cell carcinoma 1 (NY-ESO-1)] with no trials involving tumor neoepitopes. Neoepitopes, derived from non-synonymous mutations in oncogenes and primarily expressed on tumor tissues, possess strong immunogenicity and tumor heterogeneity, making neoepitopes ideal targets for cellular immunotherapy. In our earlier studies, we confirmed the cytotoxic effects of cytotoxic T lymphocytes (CTLs) induced with neoepitope-loaded dendritic cells (DCs) in HCC[13], gastric[14] and pancreatic cancers[15], indicating that neoepitope-specific CTLs are preferentially found in tumors[16]. Nevertheless, CTLs do not recognize tumor antigens as precisely as TCR-T cells, resulting in limited specific cytotoxic effects. Therefore, the current study focused on neoepitope-specific TCR-T cells, the purpose of which was to determine the role of TCR-T cells in personalized precision treatment for HCC.

Materials and methods

Patients

Sixty-seven patients with HCC were recruited from the Clinical Oncology School of Fujian Medical University (Fujian Cancer Hospital) from 2020 to 2021, 7 of whom expressed HLA-A*02:01. The diagnosis of primary HCC was verified by a minimum of two skilled pathologists. None of the patients received any therapies prior to surgical resection. The collection of tumor tissues and paired peripheral blood was approved by the Ethics Committee of the Clinical Oncology School of Fujian Medical University (Approval No. K2020-026-01). High-resolution HLA classification data of patients were analyzed by Beijing Genomics Institution (BGI) (Shenzhen, China).

Cell lines and culture

The following cell lines were graciously provided by Professor Xin Lin (Tsinghua University, Beijing, China): the human embryonic kidney cell line, Lenti-X 293T; the human hybrid B/T lymphoblastic cell line, T2 [HLA-A*02:01$^+$/transporter associated with antigen processing (TAP)$^-$]; the T2-luc cell line (HLA-A*02:01$^+$/TAP$^-$/luciferase$^+$); the human *TCR*-knockout Jurkat cell line, JC4 (TCR$^-$); and the human HCC cell lines, Huh7 (HLA-A*11:01$^+$), Huh7-luc (HLA-A*11:01$^+$/luciferase$^+$), Huh7-A2 (HLA-A*02:01$^+$), and Huh7-A2-luc (HLA-A*02:01$^+$/luciferase$^+$). The human HCC cell line, SK-HEP-1 (HLA-A*02:01$^+$), was purchased from the Cell Bank of the Chinese Academy of Sciences (Shanghai, China). Huh7-A2-neo (HLA-A*02:01$^+$/BTLA^{P267L+}), Huh7-A2-neo-luc (HLA-A*02:01$^+$/BTLA^{P267L+}/luciferase$^+$), SK-HEP-1-luc (HLA-A*02:01$^+$/luciferase$^+$), SK-HEP-1-neo (HLA-A*02:01$^+$/BTLA^{P267L+}), and SK-HEP-1-neo-luc (HLA-A*02:01$^+$/BTLA^{P267L+}/luciferase$^+$) cell lines were constructed in our laboratory. SMM 293-TII medium (M293TII; SinoBiological, Beijing, China) supplemented with 5% fetal bovine serum (FBS) (10099-141; Gibco, Carlsbad, CA, USA) was used to culture Lenti-X 293T cells. Iscove's modified Dulbecco's medium

(IMDM) (31980030; Gibco) with 20% FBS was used to culture TAP-deficient T2 and T2-luc cells. Roswell Park Memorial Institute 1640 medium (RPMI-1640) (11875085; Gibco) with 10% FBS was used to culture JC4 cells. Dulbecco's modified Eagle medium (DMEM) (C11995500BT; Gibco) with 10% FBS was used to culture Huh7 and its derived cell lines. IMDM medium with 10% FBS was used to culture SK-HEP-1 cells and its derived cell lines.

Identification of specific neoepitopes

Whole exome sequencing (WES) was performed on tumor tissues and paired peripheral blood from 7 patients with HLA-A*02:01-restricted HCC by BGI. The high-quality WES data were first matched to the human reference genome (hg38) using Burrows-Wheeler Aligner (BWA) software, then somatic mutations were called using the Mutect2 submodule of the Genome Analysis Toolkit (GATK). MuPeXI was ultimately used to predict the neoepitopes (9-mer) based on normal affinity (score < 0.001), mutant affinity (score > 0.99), and priority scores (score ≥ 99). The optimal neoepitopes were further identified by bioinformatics analyses. The filter conditions were as follows: (1) ProtParam was used to analyze the hydrophobicity of neoepitopes (available at http://web.expasy.org/protparam/). A isoelectric point (pI) < 4 was excluded. (2) Netchop3.1 was used to analyze the proteasomal cleavage probability of neoepitopes (available at https://services.healthtech.dtu.dk/services/NetChop-3.1/). Neoepitopes with three consecutive proteasomal cleavages were filtered out. (3) NetCTLpan1.1 was used to analyze the probability of neoantigens transported by TAP (available at https://services.healthtech.dtu.dk/services/NetCTLpan-1.1/). Rank ≤ 1% indicated high probability. (4) NetMHCpan4.1 was used to analyze the affinity of neoepitope to HLA-A*02:01 (available at https://services.healthtech.dtu.dk/services/NetMHCpan-4.1/). Rank < 0.5% and bind level = strong binding (SB) were included. (5) SYFPEITHI was used to analyze the affinity of neoepitope to HLA-A*02:01 (available at http://www.syfpeithi.de/0-Home.htm). Score ≥ 18 indicated high affinity. (6) Consensus was used to analyze the affinity of neoepitope to HLA-A*02:01 (available at http://tools.immuneepitope.org/main/). Score < 2 indicated high affinity. The lower the score, the higher the affinity. (7) PickPocket was used to analyze the affinity of neoepitope to HLA-A*02:01 (available at http://tools.immuneepitope.org/main/). IC_{50} ≤ 100 nM indicated high affinity. (8) NetMHCstabpan was used to analyze the stability of neoepitope-HLA-A*02:01 complexes (available at https://services.healthtech.dtu.dk/services/NetMHCstabpan-1.0/). Rank ≤ 2.5% and bind level = SB or weak binding (WB) were included. (9) A class I immunogenicity predictor was used to analyze the immunogenicity of neoepitopes (available at http://tools.iedb.org/immunogenicity/). Score > 0 indicated high immunogenicity. Neoepitopes were synthesized by GenScript (Jiangsu, China) and dissolved in dimethyl sulfoxide (DMSO) (D2438; Sigma-Aldrich, St. Louis, MO, USA). The affinity and stability of neoepitopes to HLA-A2 were further determined in the T2 cell model. T2 cells pulsed with the neoepitope (BTLA^{P267L}) and β2-microglobulin (11976-H08H; SinoBiological, Beijing, China) for 18 h were stained with FITC-labeled anti-human HLA-A2 antibody (343304, 1:200; BioLegend, San Diego, CA, USA) to detect the mean fluorescence intensity (MFI) of HLA-A2 using flow cytometry (BD, Franklin Lakes, NJ, USA). The fluorescence index (FI) was calculated as follows: (MFI of the experimental group - MFI of the control group)/MFI of the control group. A FI > 1.5 indicated strong binding affinity. T2 cells were cultured for additional 6, 12, 18, 24 or 48 h in the stability assay and the binding stability was quantified using the dissociation half-time (DC_{50}) value, which is the time necessary for 50% dissociation of the neoepitope-HLA-A2 complex that was stabilized at 0 h. A DC_{50} > 6 h indicated strong binding stability.

Identification of BTLA^{P267L}-specific TCRs

Peripheral blood mononuclear cells (PBMCs) and mitomycin C (M4287; Sigma-Aldrich)-pretreated T2 cells were co-cultured in the presence of 10 μg/mL of neoepitope BTLA^{P267L}, 3 μg/mL of β2-microglobulin, 10 ng/mL of interleukin-7 (IL-7) (HY-P7045; MCE, Monmouth Junction, NJ, USA), 10 ng/mL of IL-15 (HY-P7034; MCE), and 5 ng/mL of IL-21 (HY-P7038; MCE) for 2–3 weeks, then stained with APC-labeled tetramer (TB-7300-K2, 1:50; MBL, Minato-ku, Tokyo, Japan), FITC-labeled anti-human cluster of differentiation 8 (CD8) antibody (300906, 1:200; BioLegend, San Diego, CA, USA) and APC-Cy7-labeled anti-human eFluor™ 780 antibody (65-0865-14, 1:1000; Thermo Fisher Scientific, Waltham, MA, USA) for sorting single living CD8$^+$/tetramer$^+$ T cells using flow cytometry. Single T cell was lysed using a single-cell lysis kit (4458235; Thermo Fisher Scientific), followed by reverse transcription (18064071; Thermo Fisher Scientific) and amplification (KOD-401; Toyobo, Osaka, Japan) of the CDR3 in TCR-β and -α chains for single-cell TCR sequencing

(RuiBiotech, Beijing, China) and IgBLAST alignment (https://www.ncbi.nlm.nih.gov/igblast/). Neoepitope-specific TCRs were further identified in exogenous *TCR*-overexpressed JC4 cells by assessing infection efficiency, TCR expression rate on the cell membrane, and tetramer positivity rate using flow cytometry with 1G4 TCR targeting NY-ESO-1 as a positive control. "Infection efficiency" refers to the positive proportion of TCR-JC4 or TCR-T cells after TCR lentivirus infects JC4 or T cells. A tetramer is an artificial molecule comprised of four bound MHC molecules that specifically bind to TCRs on T cells and is widely used to detect the positive proportion of antigen-specific T cells. "Tetramer positivity rate" refers to the positive rate of T cells that specifically bind to the tetramer.

BTLA^{P267L}-specific TCR-T cell cytotoxicity

PBMCs infected with the 85-3, 126-5, or 52-3 TCR lentivirus were induced by human CD3/CD28 beads (130-111-160; Miltenyi, BGL, NRW, Germany) and IL-7/IL-15/IL-21 and 8 days later CD8$^+$ T cells were sorted using magnetic beads (130-045-201; Miltenyi), followed by tetramer staining to identify BTLA^{P267L}-specific CD8$^+$ TCR-T cells. BTLA^{P267L}-pulsed T2, SK-HEP-1-neo, SK-HEP-1-neo-luc, Huh7-A2-neo, or Huh7-A2-neo-luc cells with the corresponding control cells were cultured with BTLA^{P267L}-specific CD8$^+$ TCR-T cells to conduct the following studies: (1) Analysis of T cell markers on CD8$^+$/tetramer$^+$ TCR-T cells was performed using flow cytometry. CD8$^+$/tetramer$^+$ TCR-T cells were labeled with antibodies against 4-1BB (309810), OX40 (350008), CD28 (302912), CD25 (302630), CD69 (310910), CD107a (328620), programmed cell death protein 1 (PD-1) (379208), cytotoxic T-lymphocyte associated protein 4 (CTLA-4) (369612), interferon-gamma (IFN-γ) (502528), and tumor necrosis factor-alpha (TNF-α) (502931). All antibodies were purchased from BioLegend and diluted at a 1:200 ratio. (2) Cytotoxicity of BTLA^{P267L}-specific CD8$^+$ TCR-T cells at different effector-to-target ratios (E:T) was determined with the LDH release assay (G1780; Promega, Madison, WI, USA) or the luciferase reporter assay [for suspension cells (DD1201-02; Vazyme, Nanjing, China); for adherent cells (11401ES60; Yeasen, Shanghai, China)]. (3) IFN-γ spots produced by BTLA^{P267L}-specific CD8$^+$ TCR-T cells were detected using an ELISPOT assay (2110005; Dakewe, Shenzhen, China) and an ImmunoSPOT S6 Micro Analyzer (CTL, Shaker Heights, OH, USA). (4) IFN-γ (88-7316-88; Thermo Fisher Scientific), TNF-α (88-7346-88; Thermo Fisher Scientific), perforin (3465-1HP-2; Mabtech, Nacka Strand, STO, Sweden), or granzyme B (3486-1HP-2; Mabtech) were detected using an ELISA assay and a microplate reader (BioTek, Winooski, VT, USA).

Mouse xenograft tumor model

Female NOD/ShiLtJGpt-*Prkdc*^{em26Cd52}*Il2rg*^{em26Cd22}/Gpt (NCG) mice with severe immunodeficiency were provided by Gempharmatech Co., Ltd. (Jiangsu, China) and raised under specific pathogen-free (SPF) conditions at the Fujian Medical University Laboratory Animal Center (Fujian, China). All mice were 6–8 weeks old with a weight range of 18–20 g and had free access to food and water. SK-HEP-1-neo-luc cells (1×10^7/200 μL) were subcutaneously injected in the mid-backs of NCG mice. When the tumor volume reached 100 mm^3, CD8$^+$ TCR-T cells (5×10^6/200 μL) were injected *via* the tail vein on days 0 and 12. Luminescence was observed every 3 days using an IVIS Lumina XRMS Series III imaging system (PerkinElmer, Waltham, MA, USA), while hemocytes were collected from the orbital blood to enumerate CD8$^+$ T or CD8$^+$ TCR-T cells using flow cytometry. Plasma samples were separated to detect cytokines *via* Human CD8/NK Panel (13-plex) with V-bottom plates (741065; BioLegend). On day 33 the mice were euthanized to assess the tumor size and weight using a vernier caliper and an electronic balance. The tumor volume was calculated according to the following formula: tumor volume (mm^3) = length × width × width / 2. The primary organs (heart, liver, lungs, stomach, duodenum, kidneys, spleen, and pancreas) and xenograft tumors were dissected and hematoxylin-eosin (H&E) staining was performed. The murine experiment was approved by the Laboratory Animal Welfare and Ethics Committee of Fujian Medical University (Approval No. FJMUIACUC2021-0455).

Statistical analysis

All experiments were performed in triplicate. The Shapiro-Wilk test was used to determine the normal distribution of all quantitative data. Continuous variable measurement data were presented as the mean ± standard deviation (SD) and Student's *t*-test was utilized to evaluate the statistical difference between two groups for normal quantitative data. P values < 0.05 were considered statistically significant. Statistical analyses were performed using GraphPad Prism 9 software.

Results

Identification of specific neoepitopes with HLA-A*02:01 restriction

Ten specific neoepitopes with HLA-A*02:01 restriction were screened, of which BTLA^{P267L} (SLNHSVIGL) was detected in 3 of 7 patients and had strong water solubility, low protease cleavage probability, high transport and presentation probability, moderate stability, and strong immunogenicity (**Table S1**). The T2 cell model is commonly used in immunologic studies to assess the binding affinity of neoepitope to HLA-A2, as well as the stability of the resulting complexes. The endogenous epitopes cannot be transported to the endoplasmic reticulum (ER) to assemble with HLA-A*02:01 due to the TAP deficiency in T2 cells, which prevents subsequent processing and presentation. However, exogenous epitopes can be taken up through endocytosis and further processed *via* the endosomal-lysosomal pathway, followed by the formation of neoepitope-HLA complexes, as well as the presentation of their complexes, and finally interaction with the TCRs. The higher the affinity between the neoepitope and HLA-A2, the more stable the complexes formed, and the more these complexes are expressed on the cell surface, leading to a higher level of fluorescent expression of HLA-A2 detected by flow cytometry. It can be inferred from the FI (4.24 ± 0.35) and DC_{50} (30.33 ± 6.03 h) that BTLA^{P267L} has strong binding affinity to HLA-A2 and the complexes exhibited stable binding (**Figure S1**).

Identification of BTLA^{P267L}-specific TCR

Ninety-five percent of T cells predominantly express TCR-αβ, which includes variable and constant regions. The variable region of the TCR-β chain is encoded by the *TRBV*, *TRBD*, and *TRBJ* genes, while the TCR-α chain is encoded by *TRAV* and *TRAJ* genes. Diversity of the TCR repertoire resulting from *V(D)J* gene rearrangement helps the immune system recognize antigens and trigger immune responses, and the CDR3 domain in the variable region determines the specificity of TCR for antigen recognition. Nine specific TCR-β and paired TCR-α chain sequences targeting neoepitope BTLA^{P267L} were screened and are listed in **Table 1**.

To further verify whether these TCRs could specifically recognize neoepitope BTLA^{P267L}, endogenous *TCR*-knockout JC4 cells were infected with lentivirus encoding exogenous *TCRs*,

Table 1 BTLA^{P267L}-specific TCR sequences

Neoepitope	No.	TRBV	TRBD	TRBJ	CDR3β	TRAV	TRAJ	CDR3α
BTLA^{P267L}	9-3	TRBV27	TRBD1	TRBJ2-7	GCCAGCAGCCGAGGGACAGGGGGCTTTGAGCAGTAC	TRAV17	TRAJ33	GCTACGGACACCGATAGCAACTATCAGTTAATC
	18-1	TRBV27	TRBD1	TRBJ2-7	GCCAGCAGTTTTGGCCAGGGATCCTACGAGCAGTAC	TRAV13-2	TRAJ54	GCAGAGATCCCGGGGGGAGCCCAGAAGCTGGTA
	52-3	TRBV27	TRBD2	TRBJ2-2	GCCAGCAGTTGGGGACTTTTCACCGGGGAGCTGTTT	TRAV25	TRAJ47	GCAGGGCAGGGAGGAAACAAGCTGGTC
	82-6	TRBV27	TRBD1	TRBJ2-7	GCCAGCAGTGCCGGGACAGGGGACTACGAGCAGTAC	TRAV12-2	TRAJ27	GCCGTCCCAGGGACCAATGCAGGCAAATCAACC
	84-2	TRBV27	TRBD1	TRBJ2-7	GCCAGCAGTTCCGGGACAGGGGCCTACGAGCAGTAC	TRAV13-2	TRAJ45	GCAGAGCTATCAGGAGGAGGTGCTGACGGACTCACC
	85-3	TRBV3	TRBD1	TRBJ2-4	GCCAGCAGCCCCGGAGTGGGGGCGTACATTCAGTAC	TRAV13-2	TRAJ9	GCAGAGATCAGTGGAGGCTTCAAAACTATC
	107-3	TRBV27	TRBD1	TRBJ2-7	GCCAGCAGTTTCGGACAGGGGGCCTACGAGCAGTAC	TRAV13-2	TRAJ28	GCAGCGGGCTTGGAATCTGGGGCTGGGAGTTACCAACTCACT
	117-3	TRBV27	TRBD2	TRBJ2-7	GCCAGCAGTTTCGGGATGGGTGCCTACGAGCAGTAC	TRAV13-2	TRAJ52	GCAGAGGCTGGTGGTACTAGCTATGGAAAGCTGACA
	126-5	TRBV3	TRBD1	TRBJ2-7	GCCAGCAGCCCGGGACAGGGGGCATACGAGCAGTAC	TRAV13-2	TRAJ26	GCAGAGAATAACTATGGTCAGAATTTTGTC

TRBV, V gene of TCR-β chain; TRBD, D gene of TCR-β chain; TRBJ, J gene of TCR-β chain; CDR3β, CDR3 domain of TCR-β chain; TRAV, V gene of TCR-α chain; TRAJ, J gene of TCR-α chain; CDR3α, CDR3 domain of TCR-α chain.

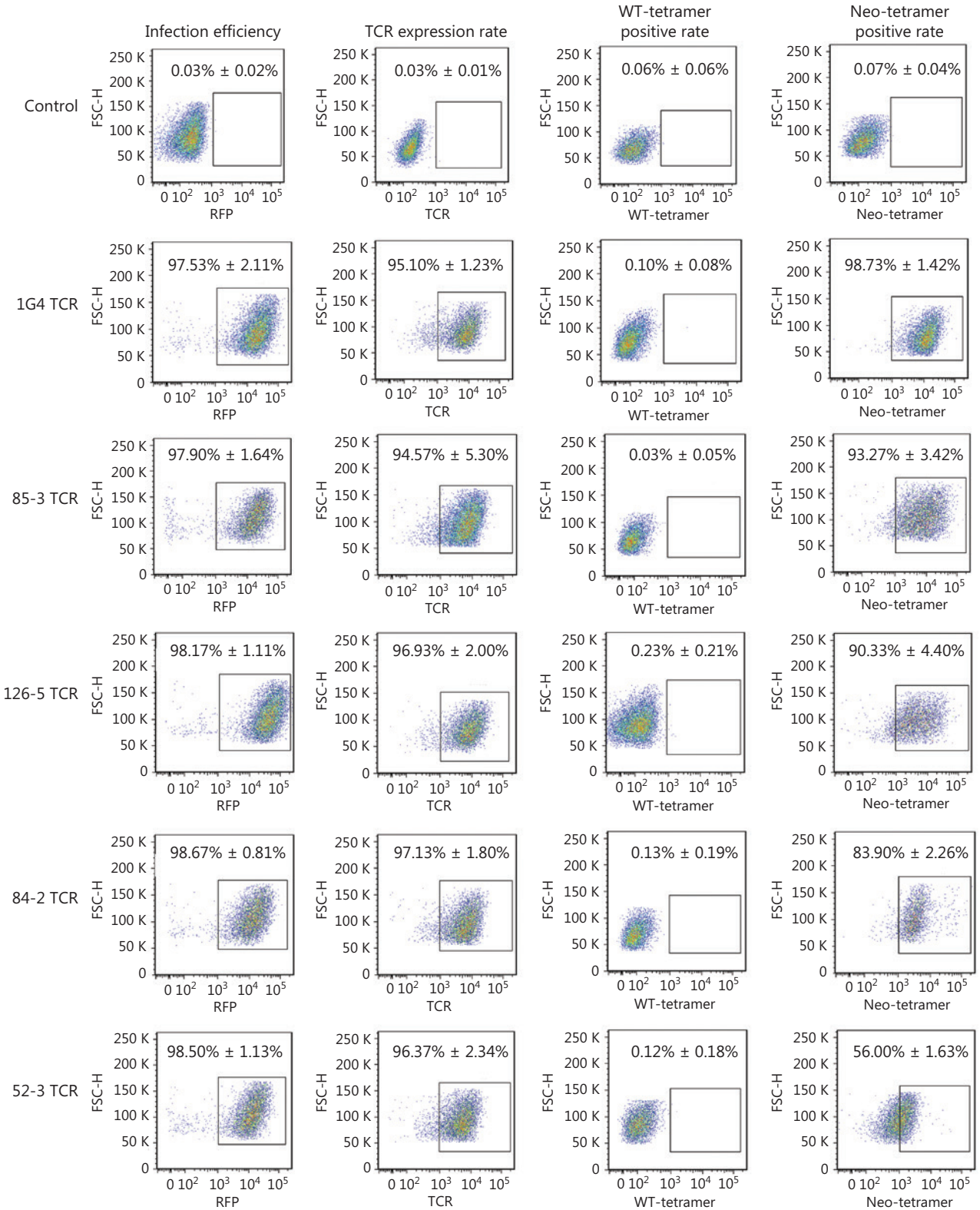


Figure 1 Continued

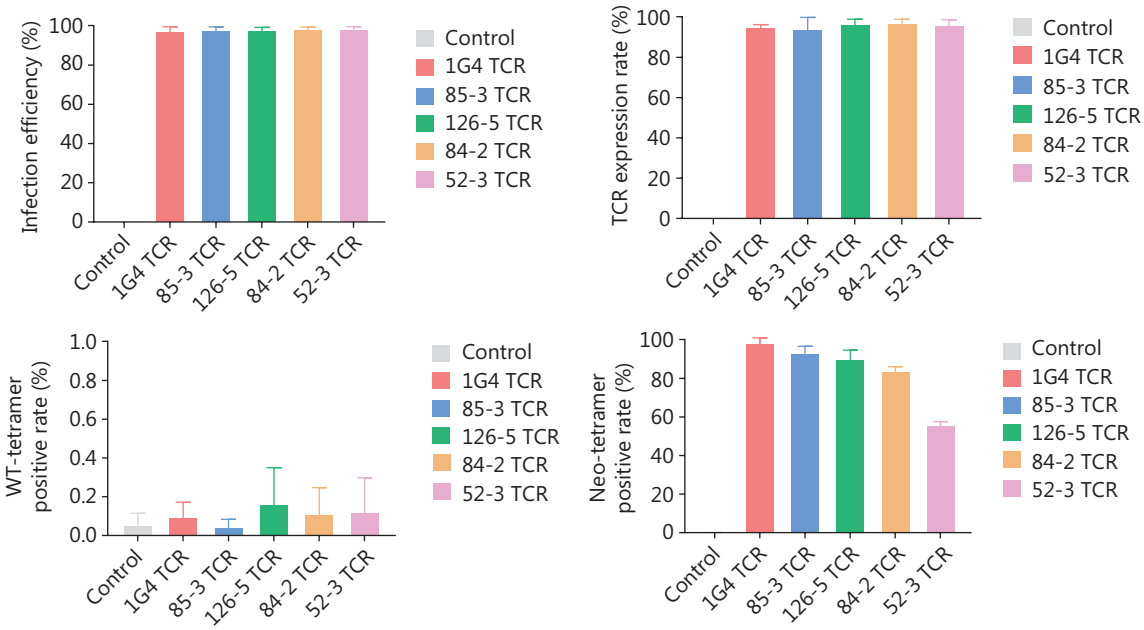


Figure 1 The infection efficiency, TCR expression rate, and tetramer-positive rate of JC4 cells. The data are displayed as the mean ± SD. RFP, red fluorescent protein; TCR, T cell receptor; WT, wild-type epitope BTLA; Neo, neoepitope BTLA^{P267L}.

effectively avoiding interference from endogenous *TCRs*. The infection efficiency of all TCR groups (except for 82-6 TCR) exceeded 95%, which was highly consistent with TCR expression. The neo-tetramer positivity rates in the TCR groups (85-3, 126-5, and 84-2) ranged from 83.90%–93.27%, while the 52-3 TCR group exhibited a lower rate of 56.00%. In addition, TCR-T cells showed extremely low WT-tetramer positive rates of 0.03%–0.23% (**Figures 1 and S2**). This finding implied that the TCRs (85-3, 126-5, and 84-2) have high specificity in recognizing BTLA^{P267L}, while the 52-3 TCR displays moderate specificity. In contrast, the other TCRs (9-3, 18-1, 82-6, 107-3, and 117-3) exhibit non-specific binding to BTLA^{P267L}.

Generation of BTLA^{P267L}-specific TCR-T cells

With prolonged culture time, TCR-T cells underwent significant expansion, nearly increasing 30-fold, and the clones continued to grow larger. On day 8, the infection efficiencies of TCR-T cells in different groups were approximately 60% and CD8$^+$/tetramer$^+$ TCR-T cell rates were (15.13% ± 6.37%) to (35.40% ± 15.91%) pre-sorting. Although the infection efficiency of 84-2 TCR-T cells approached 50%, the CD8$^+$/tetramer$^+$ TCR-T cell rate was < 2%, rendering subsequent experiments impossible. The CD8$^+$/tetramer$^+$ TCR-T cell rate showed a significant increase after magnetic bead sorting of CD8$^+$ T cells, ranking from high-to-low as 1G4 (85.07% ± 0.74%), 85-3 (53.47% ± 3.41%), 52-3 (46.07% ± 5.86%), and 126-5 (38.30% ± 11.19%) TCR-T cells (**Figure 2**). Further studies were conducted to confirm the cytotoxic effects on BTLA^{P267L}-pulsed T2 or BTLA^{P267L}-overexpressed HCC cell lines.

BTLA^{P267L}-specific CD8$^+$ TCR-T cells trigger effective cytotoxicity against BTLA^{P267L}-pulsed T2 cells

To determine the optimal concentration and incubation time for the neoepitope, T2 cells were treated with various doses of neoepitope BTLA^{P267L} for different incubation durations. The MFIs exhibited a gradual increase, positively correlated with neoepitope concentration, and reached peaks at 9 h and subsequently declined at a slower rate, suggesting that the binding of neoepitope BTLA^{P267L} to HLA-A2 was most stable at approximately 9 h (**Figure 3A**). Upon determining the optimal concentration (10 μM) and incubation time (9 h) of neoepitope to T2 cells, BTLA^{P267L}-specific CD8$^+$ TCR-T cells (abbreviated as CD8$^+$ TCR-T cells) were co-cultured with neoepitope-pulsed T2 cells to assess the cytotoxic effects of CD8$^+$ TCR-T cells. A 70%–80% specific lysis percentage at an E:T of 1:1 or 50%–70% at an E:T of 0.5:1 was observed in the LDH release assay (P < 0.001;

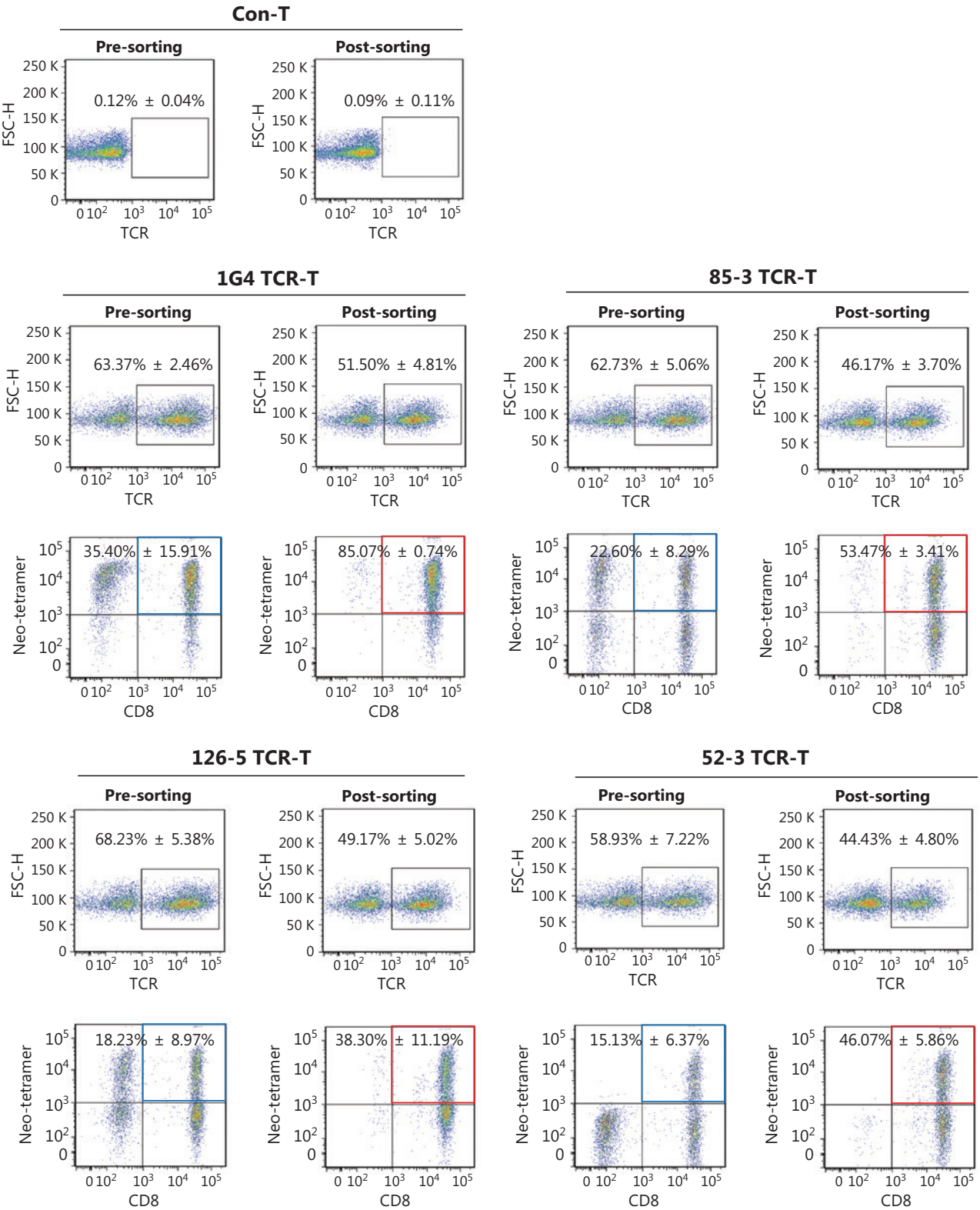


Figure 2 The infection efficiency and tetramer-positive rate of CD8$^+$ TCR-T cells pre- or post-sorting. The data are displayed as the mean ± SD.

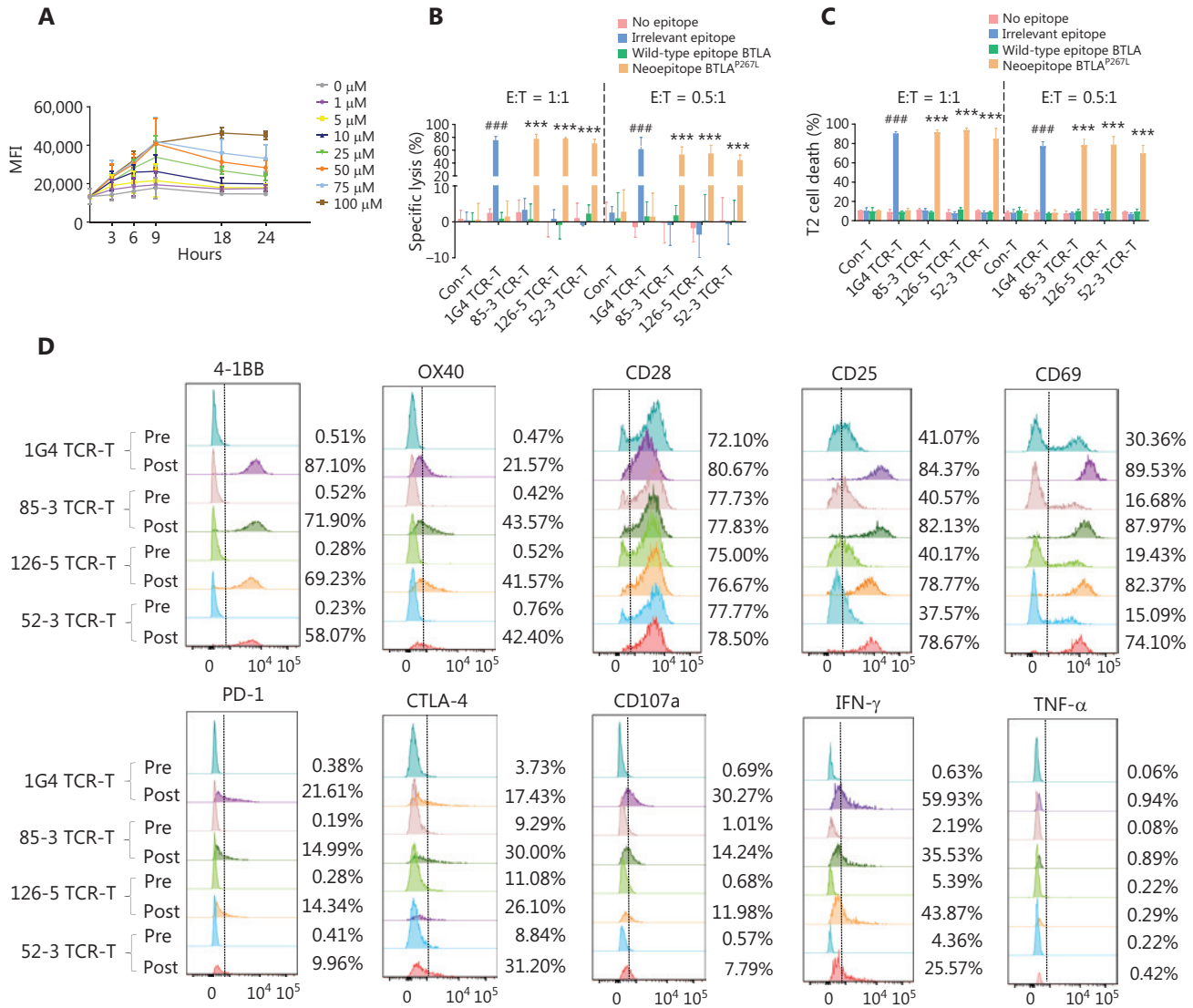


Figure 3 Cytotoxic effects of BTLA^{P267L}-specific CD8$^+$ TCR-T cells on BTLA^{P267L}-pulsed T2 cells. (A) The optimal concentration and incubation time of neoepitope BTLA^{P267L} to HLA-A2. (B) The specific lysis percentages of CD8$^+$ TCR-T cells against BTLA^{P267L}-pulsed T2 cells (E:T = 1:1 or 0.5:1). (C) T2 cell death percentages determined using a luciferase reporter assay (E:T = 1:1 or 0.5:1). (D) The T cell markers on CD8$^+$/tetramer$^+$ TCR-T cells pre- or post-coculture (E:T = 0.5:1). 1G4 TCR-T group: irrelevant epitope *vs.* other epitope groups, $^{\#\#\#}P < 0.001$; 85-3, 126-5, or 52-3 TCR-T group: neoepitope BTLA^{P267L} *vs.* other epitope groups, $^{***}P < 0.001$.

Figure 3B), which was close to the positive control (cytotoxicity of 1G4 TCR-T cells to NY-ESO-1-pulsed T2 cells). CD8$^+$ TCR-T cells showed a ≤ 10% specific lysis percentage against T2 cells pulsed with no epitope, irrelevant epitope (NY-ESO-1), or wild-type epitope BTLA. Similar tumor inhibition was observed in the luciferase reporter assay ($P < 0.001$; **Figure 3C**). The data suggest that CD8$^+$ TCR-T cells precisely recognize the neoepitope BTLA^{P267L} and kill BTLA^{P267L}-pulsed T2 cells, effectively avoiding off-tumor toxicity caused by cross-recognition.

Effective activation of TCR-T cells and the released effectors is an essential prerequisite for a potent anti-tumor response. Upregulation of 4-1BB, OX40, CD25, CD69, CD107a, IFN-γ, and PD-1 were found in CD8$^+$/tetramer$^+$ TCR-T cells ($P < 0.05$), while CD28 and TNF-α showed no significant changes. CTLA-4 had slightly different findings, with a marked increase in the 85-3 and 52-3 TCR-T groups ($P < 0.05$) but no notable change in the 126-5 group ($P > 0.05$; **Figures 3D and S3**). These findings demonstrated that the neoepitope BTLA^{P267L} effectively activates CD8$^+$

TCR-T cells while preventing excessive activation through the upregulation of PD-1 and CTLA-4. The IFN-γ spots produced by activated CD8$^+$ TCR-T cells (85-3, 126-5, or 52-3) even exceeded those of the positive control (1G4 TCR-T cells) with a decrease in the number of IFN-γ spots as the neoepitope concentration dropped. Notably, CD8$^+$ TCR-T cells secreted minimal IFN-γ when the concentration was $< 10^{-10}$ M (**Figure 4A**). Moreover, high levels of cytotoxic granules (e.g., perforin and granzyme B) and pro-inflammatory cytokines (e.g., IFN-γ and TNF-α) were detected in the co-culture supernatant ($P < 0.001$) and was positively correlated with neoepitope concentration. The 85-3 TCR-T cells produced relatively more IFN-γ and TNF-α than the other groups, whereas 126-5 TCR-T cells showed greater production of perforin and granzyme B (**Figure 4B**). These data demonstrate that BTLA^{P267L}-specific CD8$^+$ TCR-T cells are polyfunctional producers of cytotoxic granules and pro-inflammatory cytokines, triggering effective cytotoxicity against the BTLA^{P267L}-pulsed T2 cells.

BTLA^{P267L}-specific CD8$^+$ TCR-T cells exert potent cytotoxic effects on BTLA^{P267L}-overexpressed HCC cell lines

With stimulation of neoepitope BTLA^{P267L}, a greater number and larger size of CD8$^+$ TCR-T cell clones were visible in the TCR-T cells (85-3, 126-5, or 52-3) co-cultured with SK-HEP-1-neo or Huh7-A2-neo cells (**Figure 5A**), suggesting that these CD8$^+$ TCR-T cells were effectively activated by the neoepitope BTLA^{P267L} and closely related to upregulation of 4-1BB, OX40, and CD69 ($P < 0.05$). No significant changes were noted in CD28 or CD25, while IFN-γ, TNF-α, PD-1, or CTLA-4 was minimally expressed. Notably, CD107a, a cytotoxic marker, was also increased in activated CD8$^+$ TCR-T cells, which facilitated the release of cytotoxic granules (**Figures 5B and S4**). As we anticipated, CD8$^+$ TCR-T cells exerted potent cytotoxic effects on BTLA^{P267L}-overexpressed HCC cell lines ($P < 0.05$; **Figure 5C, 5D**) by releasing IFN-γ, TNF-α, perforin, and granzyme B ($P < 0.01$). IFN-γ spots produced by CD8$^+$ TCR-T cells co-cultured with Huh7-A2-neo cells were more than CD8$^+$ TCR-T cells co-cultured with SK-HEP-1-neo cells. However, the spot size in the SK-HEP-1-neo group was larger than the Huh7-A2-neo group (**Figure 5E**). Compared to 85-3 and 126-5 TCR-T cells, 52-3 TCR-T cells secreted the highest levels of IFN-γ and TNF-α, while perforin and granzyme B secretion was similar across all groups (**Figure 5F**). These findings indicate that cytotoxic granules and pro-inflammatory cytokines assist BTLA^{P267L}-specific CD8$^+$ TCR-T cells in exerting more potent cytotoxic effects on BTLA^{P267L}-overexpressed HCC cell lines.

BTLA^{P267L}-specific CD8$^+$ TCR-T cells mediate robust elimination of HCC in mice

BTLA^{P267L}-specific CD8$^+$ TCR-T cells survived for approximately 12 days following the first injection into tumor-bearing mice *via* the tail vein on day 0 (**Figure 6A, 6B**), during which the tumors grew slowly with no significant differences between CD8$^+$ TCR-T and con-T groups (con-T refers to unmodified T cells; **Figure 6C, 6D**). Three days following the second injection (day 15), CD8$^+$ TCR-T cells in the peripheral blood expanded rapidly, reaching 0.57% ± 0.34%, 0.39% ± 0.20%, and 0.67% ± 0.16% of the total circulating T cells in the 85-3, 126-5, and 52-3 TCR-T groups, respectively. In contrast, the proportion of con-T cells remained unchanged compared to that of the first injection. CD8$^+$ TCR-T cells not only experienced a notable increase in proliferation but also had a significant extension in survival time (21 days), nearly doubling that observed after the first injection (**Figure 6B**). Therefore, we concluded that CD8$^+$ TCR-T cells had a lifespan of 2–3 weeks in the peripheral circulation and the number of CD8$^+$ TCR-T cells was positively correlated with the abundance of neoepitope BTLA^{P267L}. The long-lasting survival of CD8$^+$ TCR-T cells and the substantial release of perforin ($P < 0.001$; **Figure 6F**) mediated robust elimination of HCC with the most pronounced tumor suppression in the 52-3 group ($P < 0.01$; **Figure 6C-6E**). No pathologic changes were observed in normal tissues (**Figure 6G, 6H**). A scalable workflow was displayed to illustrate the identification of neoepitope BTLA^{P267L} and corresponding TCRs, the preparation of TCR-T cells, and the validation of the anti-tumor effects *in vitro* and *in vivo* (**Figure 7**). The detailed process of neoepitope BTLA^{P267L} binding to HLA-A*02:01, the presentation of the complex on the surface of HCC cells, as well as the specific binding of BTLA^{P267L}-HLA complex to TCR, is described in **Figure 8**, thereby initiating the potent anti-tumor immune response.

Discussion

Although traditional treatments have improved the survival of patients with advanced HCC, the efficacy has not

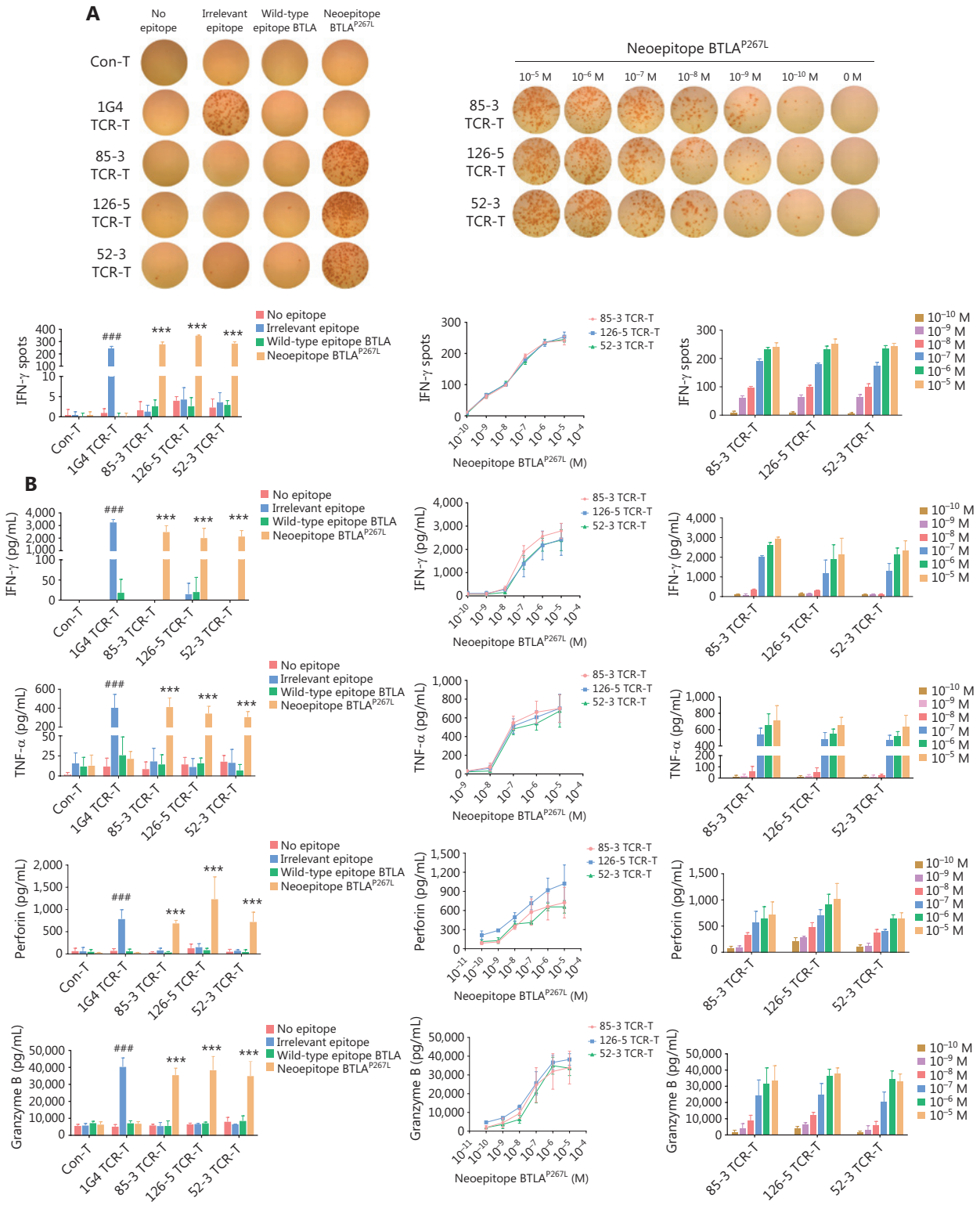


Figure 4 IFN-γ, TNF-α, perforin, and granzyme B released by BTLA^{P267L}-specific CD8$^+$ TCR-T cells. CD8$^+$ TCR-T cells were grown with different epitopes or different concentrations of BTLA^{P267L}-pulsed T2 cells for 24 h. (A) IFN-γ spots produced by CD8$^+$ TCR-T cells (E:T = 0.1:1). (B) Secretion of IFN-γ, TNF-α, perforin, and granzyme B by CD8$^+$ TCR-T cells (E:T = 0.5:1). 1G4 TCR-T group: irrelevant epitope *vs.* other epitope groups, $^{###}P < 0.001$; 85-3, 126-5, or 52-3 TCR-T group: neoepitope BTLA^{P267L} *vs.* other epitope groups, $^{***}P < 0.001$.

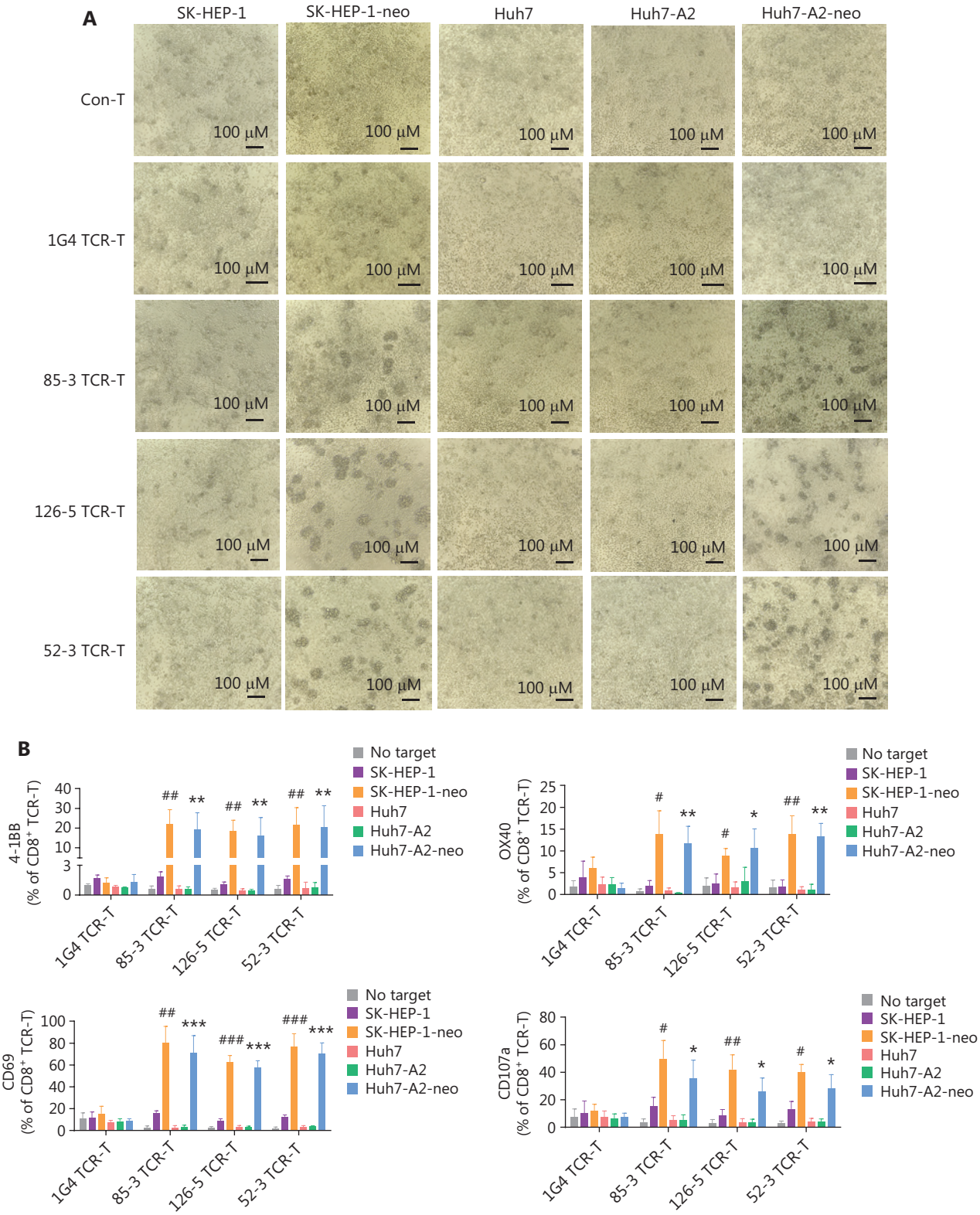


Figure 5 Continued

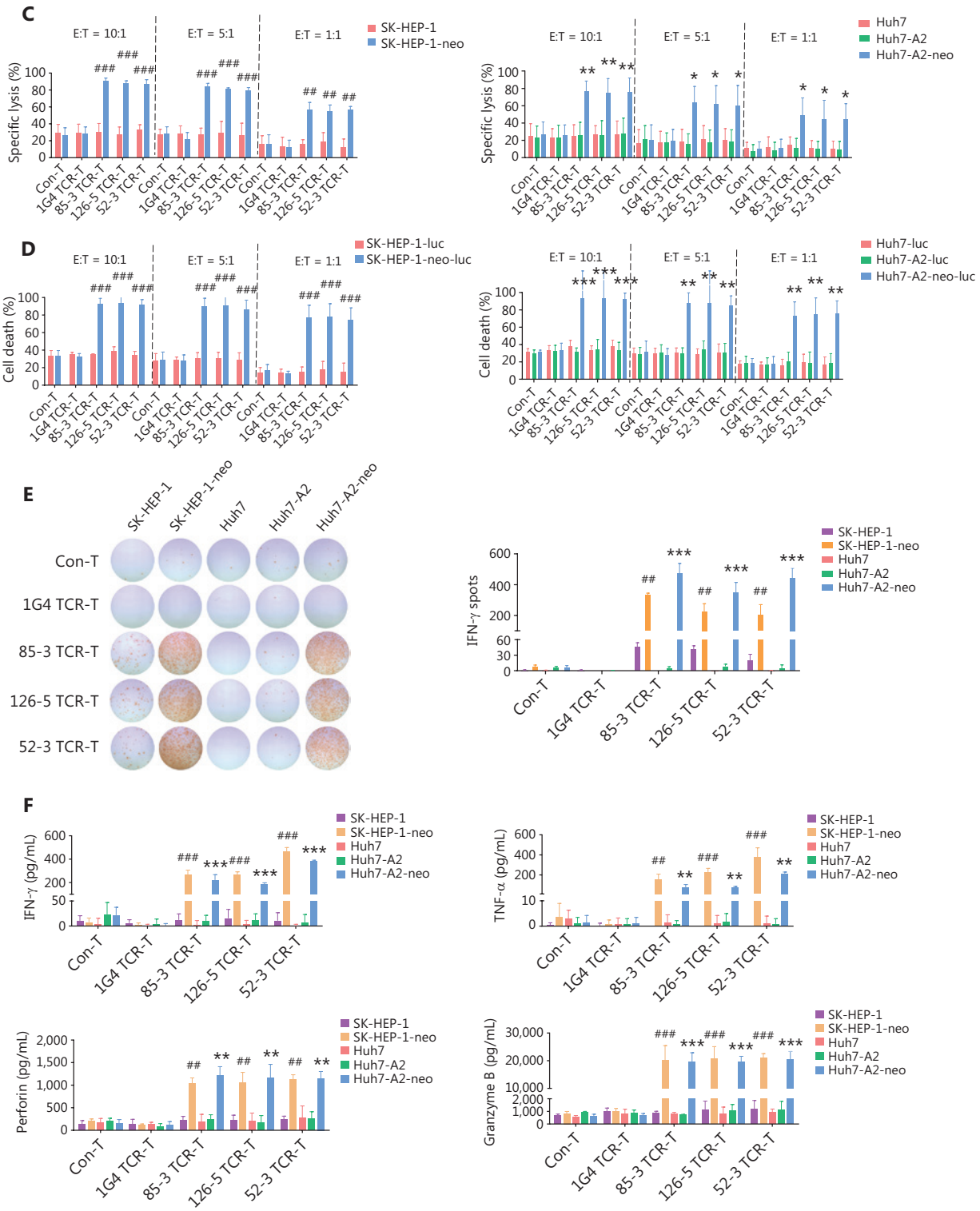


Figure 5 Cytotoxic effects of BTLA^{P267L}-specific CD8$^+$ TCR-T cells on BTLA^{P267L}-overexpressed HCC cell lines. (A) Cell morphologic changes of CD8$^+$ TCR-T cells co-cultured with HCC cell lines. Scale bar = 100 μM. (B) T cell markers expressed on CD8$^+$/tetramer$^+$ TCR-T cells (E:T = 5:1). (C) Specific lysis percentages of CD8$^+$ TCR-T cells against HCC cell lines using an LDH release assay (E:T = 10:1, 5:1, or 1:1). (D) Cell death percentages of CD8$^+$ TCR-T cells against HCC cell lines using a luciferase reporter assay (E:T = 10:1, 5:1, or 1:1). (E) IFN-γ spots produced by CD8$^+$ TCR-T cells (E:T = 3:1). (F) IFN-γ, TNF-α, perforin, and granzyme B secreted by CD8$^+$ TCR-T cells (E:T = 5:1). SK-HEP-1-neo *vs.* SK-HEP-1 or no target: $^{###}P < 0.001$, $^{##}P < 0.01$, $^{#}P < 0.05$; Huh7-A2-neo *vs.* Huh7-A2 or Huh7 or no target: $^{***}P < 0.001$, $^{**}P < 0.01$, $^{*}P < 0.05$.

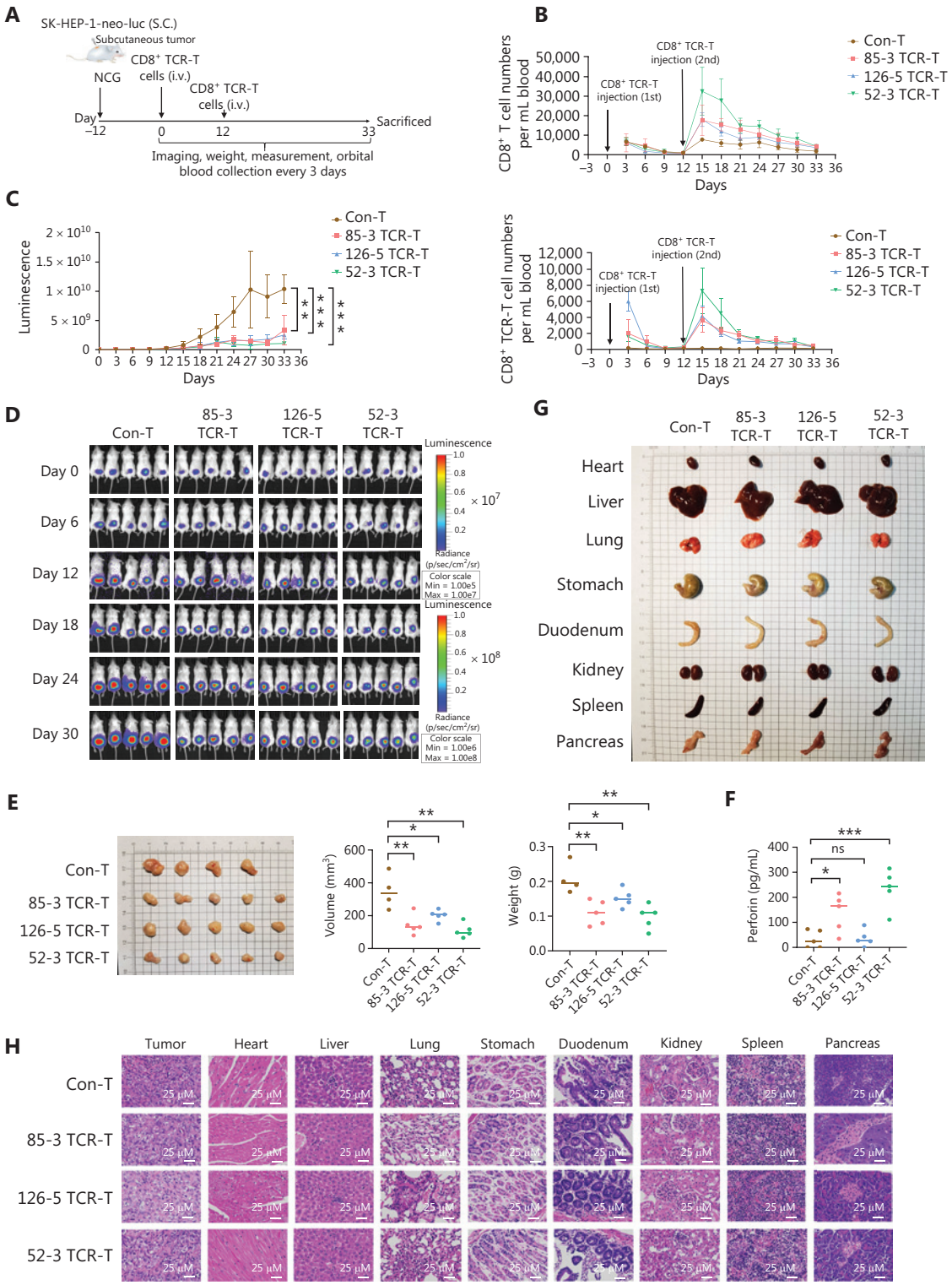


Figure 6 Anti-tumor effects of BTLA^{P267L}-specific CD8$^+$ TCR-T cells *in vivo*. (A) Flow chart of NCG murine experiments. (B) Number of circulating CD8$^+$ T cells or CD8$^+$ TCR-T cells at different times following two injections. (C) Tumor growth curve. (D) *In vivo* imaging. (E) Statistical analysis of tumor volume and weight. (F) Secretion of perforin in the peripheral blood on day 15. (G) Morphologic characteristics of eight organs in NCG mice. (H) H&E staining of transplanted tumors and organs in NCG mice. Scale bar = 25 μM; 85-3 or 126-5 or 52-3 TCR-T group *vs.* con-T group: **P* < 0.05, ***P* < 0.01, ****P* < 0.001, ns > 0.05.

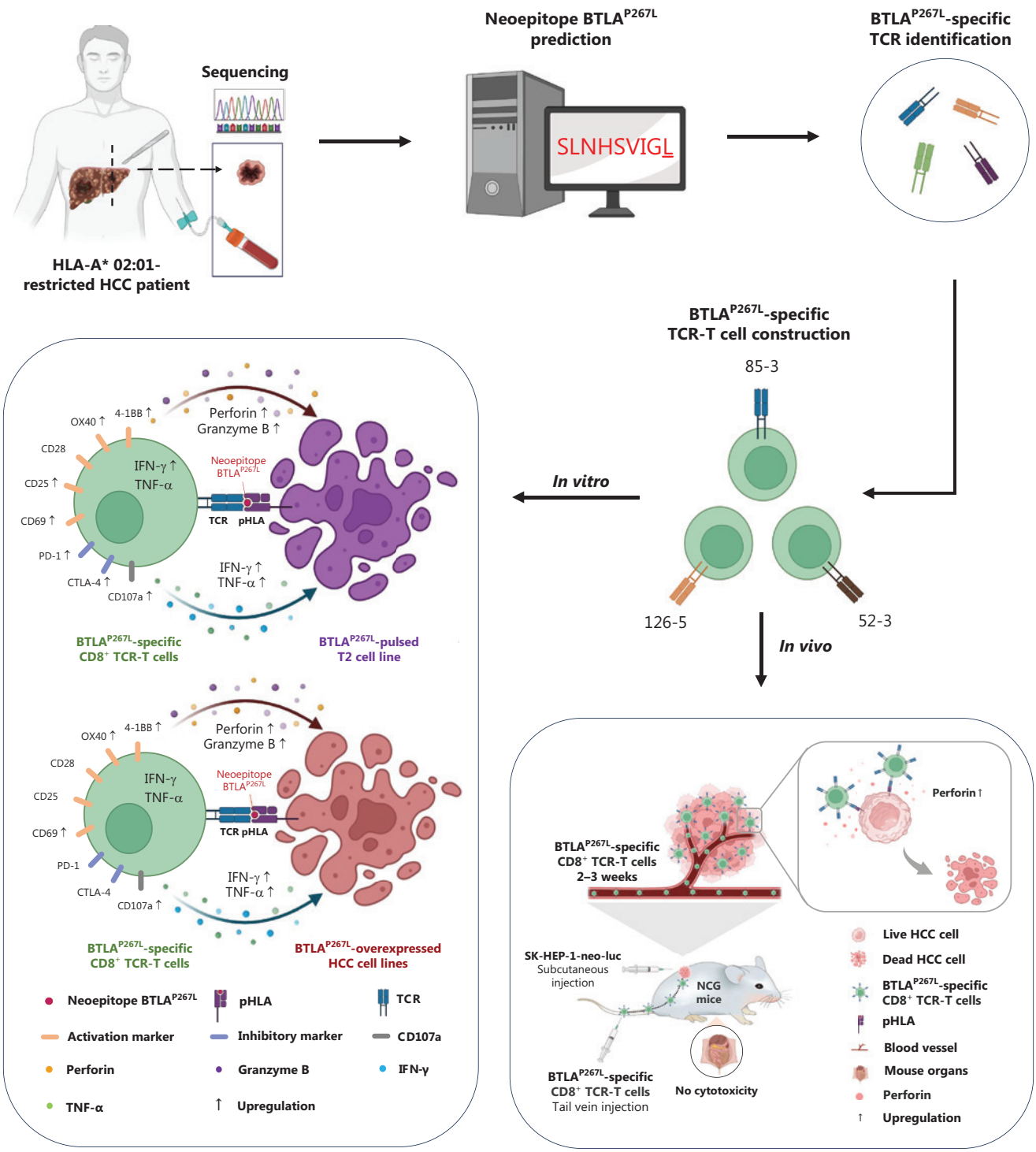


Figure 7 Continued

met expectations, resulting in a high mortality rate. Even for immunotherapy, exemplified by immune checkpoint inhibitors (ICIs), the objective response rate (ORR) of monotherapy for HCC is only 14%–20%, and dual ICIs increase it slightly to 22%–26%[17]. Nevertheless, most patients develop acquired resistance due to immune escape caused by tumor mutations or immune cell exhaustion[18]. This finding indicates that despite ICIs block the "immune brake" signals, the

Figure 7 Schematic diagram of the anti-tumor activity of BTLA^{P267L}-specific CD8$^+$ TCR-T cells. Tumor tissues and paired peripheral blood were collected from 7 patients with HLA-A*02:01-restricted HCC for WES and bioinformatics analyses, followed by identification of neoepitope BTLA^{P267L} and corresponding TCR sequences (85-3, 126-5, or 52-3) and preparation of BTLA^{P267L}-specific CD8$^+$ TCR-T cells. TAP is located on the endoplasmic reticulum and is essential for epitope presentation. Epitopes cannot be transported and presented to the membrane in T2 cells lacking TAP, and therefore cannot bind to TCR on T cells to further initiate T cell cytotoxicity. BTLA^{P267L}-pulsed T2 cells were used as target cells to exclude the interference of endogenous epitopes. While BTLA^{P267L}-specific CD8$^+$ TCR-T cells were co-cultured with exogenous BTLA^{P267L}-pulsed T2 cells or endogenous BTLA^{P267L}-overexpressed HCC cell lines, the expression of markers on activated CD8$^+$ TCR-T cells changed with the stimulation of neoepitope BTLA^{P267L}. Activation markers (CD25, CD69, 4-1BB, and OX40), inhibitory markers (PD-1 and CTLA-4) indicating feedback mechanisms in response to persistent antigen stimulation, and the cytotoxic marker (CD107a) leading to the release of cytotoxic granules (e.g., perforin and granzyme B) on the surface of CD8$^+$ TCR-T cells co-cultured with BTLA^{P267L}-pulsed T2 cells, along with the intracellular pro-inflammatory cytokine (IFN-γ) were significantly upregulated. The levels of CD69, 4-1BB, OX40, and CD107a expression were also markedly increased on the surface of CD8$^+$ TCR-T cells co-cultured with BTLA^{P267L}-overexpressed HCC cell lines. CD8$^+$ TCR-T cells activated by T2 or HCC cell lines released a large amount of pro-inflammatory cytokines (e.g., IFN-γ and TNF-α) to synergistically promote the anti-tumor effect. The murine experiments subsequently validated the results of the *in vitro* studies. SK-HEP-1-neo-luc cells were subcutaneously injected in the mid-backs of NCG mice on day -12, while BTLA^{P267L}-specific CD8$^+$ TCR-T cells (85-3, 126-5, or 52-3) were injected *via* the tail vein on days 0 and 12. CD8$^+$ TCR-T cells had a lifespan of 2–3 weeks in the peripheral circulation and mediated robust elimination of HCC by releasing perforin. The scalable workflow provides new insights for personalized precision treatment on HCC. BTLA^{P267L}, B and T lymphocyte attenuator^{P267L}; TCR, T cell receptor; HLA, human leukocyte antigen; pHLA, peptide-HLA complex; HCC, hepatocellular carcinoma; WES, whole exome sequencing; TAP, transporter associated with antigen processing; T2, human hybrid B/T lymphoblastic cell line that expresses HLA-A*02:01 but lacks TAP; ER, endoplasmic reticulum; CD, cluster of differentiation; PD-1, programmed cell death protein 1; CTLA-4, cytotoxic T-lymphocyte associated protein 4; IFN-γ, interferon-gamma; TNF-α, tumor necrosis factor-alpha; SK-HEP-1-neo-luc, hepatocellular carcinoma cell line that endogenously expresses HLA-A*02:01 and overexpresses neoepitope BTLA^{P267L} and luciferase through lentiviral infection; NCG, NOD/ShiLtJGpt-*Prkdc*^{em26Cd52}*Il2rg*^{em26Cd22}/Gpt.

fundamental anti-tumor effects rely on the immune response initiated by reactivated T cells. Patients with late-stage HCC and T-cell immune deficiency may benefit more from cellular immunotherapy and related combination treatments. Gene modified T cells, such as CAR-T or TCR-T cells, stand out as most representative and are capable of accurately recognizing tumor antigens and exerting specific cytotoxicity[19]. CAR-T therapy targeting GPC3 and AFP has shown good safety and anti-tumor efficacy in HCC treatment[3-5]. However, these targets belong to tumor-associated antigens (TAAs), which may induce off-target toxicity. Additionally, the disadvantage of CAR-T cells in recognizing tumor surface antigens makes it difficult to infiltrate into the tumor interior, and CAR-T cells are also prone to induce cytokine release syndrome (CRS), which restricts application to solid tumors. Conversely, TCR-T cells offer significant advantages in antigen recognition and infiltration into solid tumors. The unique peptide-HLA complex (pHLA)-TCR recognition mechanism endows TCR-T cells with a broad antigen recognition spectrum, allowing TCR-T cells to sensitively recognize low-abundance antigens and facilitate infiltration into solid tumors to exert effective anti-tumor effects[20]. Furthermore, the risk of CRS caused by TCR-T cells is relatively low. It is widely believed that TCR-T cell immunotherapy holds greater potential for development in the treatment of solid tumors[21].

TCR-T cell immunotherapy is an engineered T cell treatment strategy based on modifying TCR genes, which transfers the tumor antigen-specific TCR genes by viral or non-viral vectors into T cells and transfuse these amplified TCR-T cells into patients to initiate an anti-tumor response[2]. Global TCR-T cell treatment currently remains in the preclinical research or clinical trial stages and the targets mostly belong to TAAs or viral antigens[22]. In an *in vitro* study involving HCC, HBV- or HCV-specific TCR-T cells were shown to exert strong anti-tumor effects on HBV- or HCV-positive HCC cell lines by releasing IFN-γ, TNF-α, and IL-2[23,24]. In addition, novel engineered AFP-TCR-T cells armed with *IL-21* receptor against HCC further promotes memory differentiation and boosts powerful anti-tumor effects[25]. Combination therapy involving AFP-TCR-T cells also induce substantial HCC cell death by releasing IFN-γ[26]. In the mouse model, AFP-specific TCR-T cells remarkably eliminated HCC xenotransplants[27]. These findings suggest that hepatitis virus-associated proteins or AFP specifically activate the corresponding TCR-T cells, significantly inhibiting the growth of HCC. Several clinical trials involving TCR-T cells targeting HBV (NCT03899415[7,8] and NCT02719782[10]) or AFP (NCT03132792[12]) have provided promising data.

HBV-positive patients who received HBV-TCR-T cell therapy experienced significant tumor regression in the NCT03899415 trial with a disease control rate (DCR) of 66.7% and a median overall survival (OS) significantly extended to 33.1 months. No severe acute liver injury (ALI), CRS, or immune effector cell-associated neurotoxicity syndrome (ICANS) was reported. These clinical studies validated that viral antigens or TAA-targeted TCR-T cells provide a safe and effective approach for the treatment of HCC. Given the heterogeneity of HCC, customizing more precise cellular immunotherapy strategies to maximize efficacy and minimize side effects remains an ongoing goal with neoantigen-targeted TCR-T cell immunotherapy offering a solution to this challenge.

Neoantigens belong to tumor-specific antigens (TSAs) and are generated by oncogene non-synonymous mutations, including single nucleotide variations (SNVs), insertion-deletion mutations (InDels), and frameshift mutations. Because neoantigens are "non-self" antigens newly formed by tumors, the immune system recognizes neoantigens as foreign substances, triggering a strong immune response[28-30]. As early as 2014, Rosenberg[31] confirmed the high immunogenicity of neoantigens in a patient with cholangiocarcinoma. Undergoing 2 months of treatment with neoantigen ERBB2IP^{E805G}-activated T cells, all tumor lesions regressed, showing a 30% reduction 7 months later and stability for 13 months[31]. Therefore, neoantigens with high immunogenicity and tumor specificity have gained considerable attention. As a critical fragment of the neoantigen, the neoepitope is typically 8–11 amino acids in length and holds paramount importance in triggering a specific immune response[32]. The rapid advances in next-generation sequencing and bioinformatic prediction tools have facilitated the decoding of tumor neoepitopes, which provide specific targets for precise tumor treatment.

In the current study, a scalable workflow was developed and a specific neoepitope BTLA^{P267L} (SLNHSVIGL) was identified in 3 of 7 patients with high antigen presentation probability and strong immunogenicity. BTLA (CD272) is a co-inhibitory receptor and a member of the CD28/B7 superfamily that is highly expressed in various tumors and significantly associated with a poor prognosis[33-35], implying that BTLA^{P267L} is a promising tumor target for cellular immunotherapy. Previous studies have proved that neoepitope BTLA^{P267L}-specific CTLs activated by BTLA^{P267L}-loaded DCs exert potent anti-tumor effects against BTLA^{P267L}-overexpressed HCC cell lines. TCR-T cells aroused our interest due to the greater tumor specificity and stronger cytotoxic effects over CTLs. The potent anti-tumor effects of neoepitope-targeted TCR-T cells on multiple types of solid tumors have been reported, such as melanoma[36], metastatic colorectal cancer[37], pancreatic cancer[38], and metastatic HPV16-positive epithelial tumors[39]. As of January 2025, no clinical trials related to neoepitope-targeted TCR-T cells on HCC have been conducted in the US Clinical Trial Database (https://clinicaltrials.gov) or the Chinese Clinical Trial Registry (https://www.chictr.org.cn), which prompted us to conduct in-depth research.

The prerequisite for TCR-T cells to recognize tumor antigens and initiate immune responses is based on a vast TCR repertoire (10^{16}–10^{18}) that results from *V(D)J* gene rearrangement[40]. Another notable feature of TCRs is that a single TCR clone can recognize multiple epitopes. Conversely, a single epitope can also be recognized by multiple TCR clones with the CDR3 loop being highly variable and responsible for epitope recognition[41]. Due to immune tolerance or immunodeficiency in patients with tumors, the types and quantities of TCRs specifically recognizing tumor neoepitopes are markedly reduced. Therefore, we identified neoepitope-specific TCRs from healthy donors with more diversity of TCR clones. For the neoepitope BTLA^{P267L}, three specific TCR clones (85-3, 126-5, and 52-3) were identified, among which the 85-3 and 126-5 sequences were quite similar with only slight differences in the *J* gene and CDR3 domain, whereas 52-3 TCR showed greater dissimilarity to the former two sequences. Structural differences in TCRs may influence binding to pHLA complexes, leading to variations in the anti-tumor function of TCR-T cells.

When the BTLA^{P267L}-specific TCRs lock onto the BTLA^{P267L}-HLA complexes, notable increases in the activation (CD25, CD69, 4-1BB, and OX40) and inhibitory markers (PD-1 and CTLA-4) indicate feedback mechanisms in response to persistent antigen stimulation. The cytotoxic marker, CD107a, leading to the release of cytotoxic granules were observed on the activated BTLA^{P267L}-specific CD8$^+$ TCR-T cells, accompanied by a substantial release of cytotoxic granules (perforin and granzyme B) and pro-inflammatory cytokines (IFN-γ and TNF-α) in a dose-dependent manner. With support of these factors, BTLA^{P267L}-specific CD8$^+$ TCR-T cells exhibited strong cytotoxicity against BTLA^{P267L}-pulsed T2 cells or BTLA^{P267L}-overexpressed HCC cell lines even at low effector-to-target ratios, while no cross-recognition of wild-type or irrelevant epitope was detected, effectively avoiding off-target toxicity. In addition, an interesting finding caught our attention. Although the infection efficiency and TCR expression rate in the 52-3 group were not as high as those in the other two groups and the

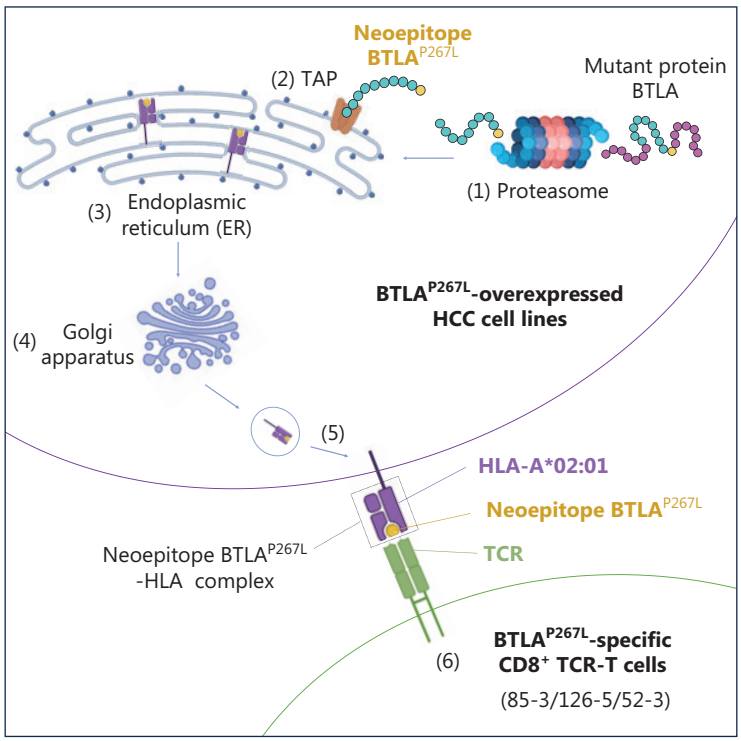


Figure 8 Schematic diagram of neoepitope presentation by HLA and the specific binding of TCR to BTLA^{P267L}-HLA complex. (1) The mutant proteins BTLA were degraded into smaller neoepitope fragments by proteasomes. (2) The neoepitopes (BTLA^{P267L}) were transported into the lumen of ER by TAP located on the ER membrane. (3) The HLA-A*02:01 molecules were assembled with the neoepitopes (BTLA^{P267L}) in the ER lumen. (4) The BTLA^{P267L}-HLA complexes were transported to the Golgi apparatus for further processing, where the complexes were glycosylated to enhance structural stability and further folded to ensure accurate display of the neoepitope (BTLA^{P267L}) for TCR binding. (5) The BTLA^{P267L}-HLA complexes were then transported to the cell surface *via* vesicular trafficking. (6) The BTLA^{P267L}-HLA complexes were bound to 85-3, 126-5, or 52-3 TCR, subsequently triggering specific tumor killing by the corresponding TCR-T cells. All three TCRs specifically targeted the same neoepitope (BTLA^{P267L}), however, the binding site and affinity differed slightly. HLA, human leukocyte antigen; TCR, T cell receptor; BTLA^{P267L}, B and T lymphocyte attenuator^{P267L}; ER, endoplasmic reticulum; TAP, transporter associated with antigen processing.

affinity of TCR to BTLA^{P267L}-HLA-A*02:01 complex was also inferior to that in the 85-3 group, the 52-3 TCR-T cells released the largest amount of cytotoxic granules and pro-inflammatory cytokines, thereby triggering the strongest anti-tumor effect on BTLA^{P267L}-overexpressed HCC cell lines. The anti-tumor functional differences of TCR-T cells are closely related to the TCR structural features. The shape complementarity (SC) between the TCR and pHLA complex directly affects binding affinity and stability. The types of amino acid residues, the arrangement, polar interactions between residues, as well as the binding angle and contact area, all affect the SC, thereby altering the binding duration. The binding duration between TCR and pHLA usually ranges from several hundred milliseconds to several minutes. The longer the binding duration, the better the stimulation and activation of T cells, leading to a stronger anti-tumor response[42,43]. We speculate that 52-3 TCR achieves better SC with BTLA^{P267L}-HLA-A*02:01 complex and an appropriate affinity might be more beneficial in inducing immune responses; conversely, higher affinity more likely causes premature T cell exhaustion. This finding was further validated in murine experiments. Even though the proportion of 52-3 CD8$^+$ TCR-T cells was < 1%, significant tumor regression was triggered that was closely related to the long-term survival of CD8$^+$ TCR-T cells, as well as the massive release of perforin. Concurrently, no cytotoxicity on normal organs was demonstrated in murine experiments, which indicated that the application of CD8$^+$ TCR-T cells on HCC is safe. Chen et al.[44] also reported similar findings by identifying two specific neoepitopes (FYAFSCYYDL and WVWCMSPTI restricted by HLA-A*24:02 and HLA-A*02:01, respectively). A dominant TCR clone (S20-1-BA) targeting FYAFSCYYDL was identified, corresponding to the neoantigen ENTPD6. Strong tumor

suppression caused by intratumoral injection of ENTPD6-specific TCR-T cells was also observed in tumor-bearing mice. The difference from our study was that Chen et al.[44] administered TCR-T cells *via* intratumoral injection, whereas we employed tail vein injection, which more accurately mimics clinical application. Additionally, the tumor suppression observed from our two consecutive injections of TCR-T cells appeared to be superior to their three consecutive injections. TCR-T cell therapy targeting neoepitopes holds promising prospects for the treatment of HCC.

With the advances in technology, refinement of TCR-T cell therapy also requires additional efforts in the future, such as developing more precise neoepitope prediction platforms based on artificial intelligence (AI), enhancing TCR affinity through genetic modification[45-47], and engineering tumor cells to express a variety of HLA molecules or developing non-HLA-dependent TCR-T cells to circumvent issues of HLA restriction[48-51]. Potential off-target risks of TCR-T cells deserve special attention, such as tumor antigens misrecognition caused by TCR mismatches or cross-reactivity of TCR with both target and non-target antigens. These risks may induce adverse events, such as CRS, cardiac toxicity, ocular toxicity, skin toxicity, auditory damage, or severe acute colitis. TCR mismatches were caused by the incorrect pairing of TCR-α and TCR-β or the mismatches of endogenous TCR chains with exogenous chains. This issue could be resolved by knocking out endogenous TCRs or modifying the human TCR constant region into a murine form. Additionally, the use of bioinformatics tools to predict the binding properties of TCRs to target or non-target antigens and further preclinical model validation can help avoid potential cross-reactivity. In the event of off-target toxicity, the use of "logic gate strategy" or "safety switch" is also a good strategy to quickly clear TCR-T cells[6,52]. The development strategy of neoepitope-targeted TCR-T cells demonstrates immense potential for clinical application and provides a clear direction for future research.

Conclusions

Based on sequencing data sourced from tumor tissue and peripheral blood of patients with HCC, we developed a rapid and scalable workflow aimed at identifying personalized neoepitopes and their corresponding TCRs to further validate potent anti-tumor effects of $CD8^+$ TCR-T cells and unlock new personalized precision treatment for HCC. In the future, we will expand the scalable workflow to other HLA types commonly found in the Chinese population and establish TCR libraries targeting multiple neoepitopes to further explore clinical applications.

Grant support

This work was supported by grants from the Joint Funds for the Innovation of Science and Technology of Fujian Province (Grant No. 2018Y9108 and 2024Y9607), the Natural Science Foundation of Fujian Province (Grant No. 2023J011247), the Science and Technology Project of Fujian Province (Grant No. 2021Y0054), and the Fujian Provincial Health Technology Project (Grant No. 2020GGA018).

Conflict of interest statement

No potential conflicts of interest are disclosed.

Author contributions

Conceived and designed the analysis: Yunbin Ye, Xueqiang Zhao, Xin Lin, Wei Rui, Fang Liu.
Collected the data: Fang Liu, Suxin Wu, Chenlu Zhu, Mingji Zhang, Dong Zhou.
Contributed data or analysis tools: Fang Liu, Suxin Wu, Yang Wang.
Performed the analysis: Fang Liu, Hua Chen, Suxin Wu.
Wrote the manuscript: Fang Liu, Yunbin Ye.

Data availability statement

Data were generated by the authors and available on request.

References

1. Han B, Zheng R, Zeng H, Wang S, Sun K, Chen R, et al. Cancer incidence and mortality in China, 2022. J Natl Cancer Cent. 2024; 4: 47-53.
2. Lee SW, Lee HM. Engineered T cell receptor for cancer immunotherapy. Biomol Ther (Seoul). 2024; 32: 424-31.
3. Li D, Qin J, Zhou T, Li Y, Cheng X, Chen Z, et al. Bispecific GPC3/PD-1 CAR-T cells for the treatment of HCC. Int J Oncol. 2023; 62: 1-10.
4. Lu LL, Xiao SX, Lin ZY, Bai JJ, Li W, Song ZQ, et al. GPC3-IL7-CCL19-CAR-T primes immune microenvironment reconstitution for hepatocellular carcinoma therapy. Cell Biol Toxicol. 2023; 39: 3101-19.
5. Wang Y, Zhao Y, Li M, Hou H, Jian Z, Li W, et al. Conversion of primary liver cancer after targeted therapy for liver cancer

combined with AFP-targeted CAR T-cell therapy: a case report. Front Immunol. 2023; 14: 1180001.
6. Baulu E, Gardet C, Chuvin N, Depil S. TCR-engineered T cell therapy in solid tumors: state of the art and perspectives. Sci Adv. 2023; 9: eadf3700.
7. Meng F, Zhao J, Tan AT, Hu W, Wang SY, Jin J, et al. Immunotherapy of HBV-related advanced hepatocellular carcinoma with short-term HBV-specific TCR expressed T cells: results of dose escalation, phase I trial. Hepatol Int. 2021; 15: 1402-12.
8. Tan AT, Meng F, Jin J, Zhang JY, Wang SY, Shi L, et al. Immunological alterations after immunotherapy with short lived HBV-TCR T cells associates with long-term treatment response in HBV-HCC. Hepatol Commun. 2022; 6: 841-54.
9. Parayath NN, Stephan SB, Koehne AL, Nelson PS, Stephan MT. In vitro-transcribed antigen receptor mRNA nanocarriers for transient expression in circulating T cells in vivo. Nat Commun. 2020; 11: 6080.
10. Yang F, Zheng X, Koh S, Lu J, Cheng J, Li P, et al. Messenger RNA electroporated hepatitis B virus (HBV) antigen-specific T cell receptor (TCR) redirected T cell therapy is well-tolerated in patients with recurrent HBV-related hepatocellular carcinoma post-liver transplantation: results from a phase I trial. Hepatol Int. 2023; 17: 850-9.
11. Luo X, Cui H, Cai L, Zhu W, Yang WC, Patrick M, et al. Selection of a clinical lead TCR targeting alpha-fetoprotein-positive liver cancer based on a balance of risk and benefit. Front Immunol. 2020; 11: 623.
12. Goyal L, Frigault M, Meyer T, Feun LG, Bruix J, El-Khoueiry A, et al. Abstract 3183: initial safety of AFP SPEAR T-cells in patients with advanced hepatocellular carcinoma. Cancer Res. 2019; 79: 3183.
13. Ye C, Lin S, Hong J, Liu F, Guo G, Chen S, et al. Altered HLA-A2-restricted TP53 epitope induces specific CTL cytotoxicity against hepatocellular carcinoma. Eur J Immunol. 2023; 53: e2250054.
14. Yu H, Li J, Yuan Y, Chen Y, Hong J, Ye C, et al. Residue substitution enhances the immunogenicity of neoepitopes from gastric cancers. Cancer Biol Med. 2021; 18: 1053-64.
15. Lin S, Hong J, Wu S, Zhu C, Liu F, Lin W, et al. BCL2A1 neoepitopes-elicited cytotoxic T lymphocytes are a promising individualized immunotherapy of pancreatic cancer. J Leukoc Biol. 2024; 1-31.
16. Schmidt J, Chiffelle J, Perez MAS, Magnin M, Bobisse S, Arnaud M, et al. Neoantigen-specific CD8 T cells with high structural avidity preferentially reside in and eliminate tumors. Nat Commun. 2023; 14: 3188.
17. Scheiner B, Roessler D, Phen S, Lim M, Pomej K, Pressiani T, et al. Efficacy and safety of immune checkpoint inhibitor rechallenge in individuals with hepatocellular carcinoma. JHEP Rep. 2023; 5: 100620.
18. Sun L, Yang Y, Li Y, Li Y, Zhang B, Shi R. The past, present, and future of liver cancer research in China. Cancer Lett. 2023; 574: 216334.
19. Mody H, Ogasawara K, Zhu X, Miles D, Shastri PN, Gokemeijer J, et al. Best practices and considerations for clinical pharmacology and pharmacometric aspects for optimal development of CAR-T and TCR-T cell therapies: an industry perspective. Clin Pharmacol Ther. 2023; 114: 530-57.
20. Ma P, Jiang Y, Zhao G, Wang W, Xing S, Tang Q, et al. Toward a comprehensive solution for treating solid tumors using T-cell receptor therapy: a review. Eur J Cancer. 2024; 209: 114224.
21. Drakes DJ, Abbas AM, Shields J, Steinbuck MP, Jakubowski A, Seenappa LM, et al. Lymph node-targeted vaccine boosting of TCR T-cell therapy enhances antitumor function and eradicates solid tumors. Cancer Immunol Res. 2024; 12: 214-31.
22. Shao W, Yao Y, Yang L, Li X, Ge T, Zheng Y, et al. Novel insights into TCR-T cell therapy in solid neoplasms: optimizing adoptive immunotherapy. Exp Hematol Oncol. 2024; 13: 37.
23. Ma Y, Ou J, Lin T, Chen L, Chen J, Wang M. Next generation sequencing-based identification of T-cell receptors for immunotherapy against hepatocellular carcinoma. Hepatol Commun. 2021; 5: 1106-19.
24. Silva DN, Chrobok M, Rovesti G, Healy K, Wagner AK, Maravelia P, et al. Process development for adoptive cell therapy in academia: a pipeline for clinical-scale manufacturing of multiple TCR-T cell products. Front Immunol. 2022; 13: 896242.
25. Zhu W, Zhang Z, Chen J, Chen X, Huang L, Zhang X, et al. A novel engineered IL-21 receptor arms T-cell receptor-engineered T cells (TCR-T cells) against hepatocellular carcinoma. Signal Transduct Target Ther. 2024; 9: 101.
26. Chen A, Yu Z, Ma N, Lu X, Zhang Y, Xu W, et al. Atovaquone enhances antitumor efficacy of TCR-T therapy by augmentation of ROS-induced ferroptosis in hepatocellular carcinoma. Cancer Immunol Immunother. 2024; 73: 49.
27. Cai L, Caraballo Galva LD, Peng Y, Luo X, Zhu W, Yao Y, et al. Preclinical studies of the off-target reactivity of AFP158-specific TCR engineered T cells. Front Immunol. 2020; 11: 607.
28. Guan H, Wu Y, Li LU, Yang Y, Qiu S, Zhao Z, et al. Tumor neoantigens: novel strategies for application of cancer immunotherapy. Oncol Res. 2023; 31: 437-48.
29. Ho SY, Chang CM, Liao HN, Chou WH, Guo CL, Yen Y, et al. Current trends in neoantigen-based cancer vaccines. Pharmaceuticals (Basel). 2023; 16: 392.
30. Li X, You J, Hong L, Liu W, Guo P, Hao X. Neoantigen cancer vaccines: a new star on the horizon. Cancer Biol Med. 2023; 21: 274-311.
31. Tran E, Turcotte S, Gros A, Robbins PF, Lu YC, Dudley ME, et al. Cancer immunotherapy based on mutation-specific CD4+ T cells in a patient with epithelial cancer. Science. 2014; 344: 641-5.
32. Gurung HR, Heidersbach AJ, Darwish M, Chan PPF, Li J, Beresini M, et al. Systematic discovery of neoepitope-HLA pairs for neoantigens shared among patients and tumor types. Nat Biotechnol. 2023; 42: 1107-17.
33. Wojciechowicz K, Spodzieja M, Wardowska A. The BTLA-HVEM complex – The future of cancer immunotherapy. Eur J Med Chem. 2024; 268: 116231.
34. Cao R, Tang W, Chen S. Association between BTLA polymorphisms and susceptibility to esophageal squamous cell carcinoma in the Chinese population. J Clin Lab Anal. 2020; 34: e23221.

35. Jiang X, He J, Wang Y, Liu J, Li X, He X, et al. A pan-cancer analysis of the biological function and clinical value of BTLA in tumors. Biocell. 2023; 47: 351-66.
36. Puig-Saus C, Sennino B, Peng S, Wang CL, Pan Z, Yuen B, et al. Neoantigen-targeted CD8$^+$ T cell responses with PD-1 blockade therapy. Nature. 2023; 615: 697-704.
37. Lo W, Parkhurst M, Robbins PF, Tran E, Lu YC, Jia L, et al. Immunologic recognition of a shared p53 mutated neoantigen in a patient with metastatic colorectal cancer. Cancer Immunol Res. 2019; 7: 534-43.
38. Leidner R, Sanjuan Silva N, Huang H, Sprott D, Zheng C, Shih YP, et al. Neoantigen T-cell receptor gene therapy in pancreatic cancer. N Engl J Med. 2022; 386: 2112-9.
39. Doran SL, Stevanović S, Adhikary S, Gartner JJ, Jia L, Kwong MLM, et al. T-cell receptor gene therapy for human papillomavirus-associated epithelial cancers: a first-in-human, phase I/II study. J Clin Oncol. 2019; 37: 2759-68.
40. Chen L, Hu Y, Zheng B, Luo L, Su Z. Human TCR repertoire in cancer. Cancer Med. 2024; 13: e70164.
41. Yao Z, Zeng Y, Liu C, Jin H, Wang H, Zhang Y, et al. Focusing on CD8$^+$ T-cell phenotypes: improving solid tumor therapy. J Exp Clin Cancer Res. 2024; 43: 266.
42. Lanz AL, Masi G, Porciello N, Cohnen A, Cipria D, Prakaash D, et al. Allosteric activation of T cell antigen receptor signaling by quaternary structure relaxation. Cell Rep. 2021; 36: 109375.
43. Sušac L, Vuong MT, Thomas C, Von Bulow S, O'brien-Ball C, Santos AM, et al. Structure of a fully assembled tumor-specific T cell receptor ligated by pMHC. Cell. 2022; 185: 3201-13.e3219.
44. Chen P, Chen D, Bu D, Gao J, Qin W, Deng K, et al. Dominant neoantigen verification in hepatocellular carcinoma by a single-plasmid system coexpressing patient HLA and antigen. J Immunother Cancer. 2023; 11: e006334.
45. Hiltensperger M, Krackhardt AM. Current and future concepts for the generation and application of genetically engineered CAR-T and TCR-T cells. Front Immunol. 2023; 14: 1121030.
46. Foy SP, Jacoby K, Bota DA, Hunter T, Pan Z, Stawiski E, et al. Non-viral precision T cell receptor replacement for personalized cell therapy. Nature. 2022; 615: 687-96.
47. Sun Y, Li F, Sonnemann H, Jackson KR, Talukder AH, Katailiha AS, et al. Evolution of CD8$^+$ T cell receptor (TCR) engineered therapies for the treatment of cancer. Cells. 2021; 10: 2379.
48. Dolton G, Rius C, Wall A, Szomolay B, Bianchi V, Galloway SAE, et al. Targeting of multiple tumor-associated antigens by individual T cell receptors during successful cancer immunotherapy. Cell. 2023; 186: 3333-49.e3327.
49. Klebanoff CA, Chandran SS, Baker BM, Quezada SA, Ribas A. T cell receptor therapeutics: immunological targeting of the intracellular cancer proteome. Nat Rev Drug Discov. 2023; 22: 996-1017.
50. Pang Z, Lu MM, Zhang Y, Gao Y, Bai JJ, Gu JY, et al. Neoantigen-targeted TCR-engineered T cell immunotherapy: current advances and challenges. Biomark Res. 2023; 11: 104.
51. Xu R, Wang Q, Zhu J, Bei Y, Chu Y, Sun Z, et al. Membrane fusogenic nanoparticle-based HLA-peptide-addressing universal T cell receptor-engineered T (HAUL TCR-T) cell therapy in solid tumor. Bioeng Transl Med. 2023; 8: e10585.
52. Zhao Q, Jiang Y, Xiang S, Kaboli PJ, Shen J, Zhao Y, et al. Engineered TCR-T cell Immunotherapy in anticancer precision medicine: pros and cons. Front Immunol. 2021; 12: 658753.

Cite this article as: Liu F, Chen H, Wu S, Zhu C, Zhang M, Rui W, et al. Neoepitope BTLA^{P267L}-specific TCR-T cell immunotherapy unlocks precision treatment for hepatocellular carcinoma. Cancer Biol Med. 2025; 22: 412-432. doi: 10.20892/j.issn.2095-3941.2024.0434